

1 Supplemental Information for
2 **Evolution of Organic Carbon in the Laboratory Oxidation of**
3 **Biomass Burning Emissions**
4

5 Kevin J. Nihill,^{1,a} Matthew M. Coggon,^{2,3} Christopher Y. Lim,^{1,b} Abigail R. Koss,^{2,3,4,c}
6 Bin Yuan,^{2,3,d} Jordan E. Krechmer,^{3,4,e} Kanako Sekimoto,^{2,3,5} Jose L. Jimenez,^{3,4}
7 Joost de Gouw,^{2,3,4} Christopher D. Cappa,⁶ Colette L. Heald,^{1,7} Carsten Warneke,^{2,3}
8 Jesse H. Kroll^{1,8}
9

10 ¹ Department of Civil and Environmental Engineering, Massachusetts Institute of Technology, Cambridge, MA,
11 USA

12 ² NOAA Chemical Sciences Laboratory, Boulder, CO, USA

13 ³ Cooperative Institute for Research in Environmental Sciences, University of Colorado, Boulder, CO, USA

14 ⁴ Department of Chemistry, University of Colorado, Boulder, CO, USA

15 ⁵ Graduate School of Nanobioscience, Yokohama City University, Yokohama, Kanagawa, Japan

16 ⁶ Department of Civil and Environmental Engineering, University of California, Davis, CA, USA

17 ⁷ Department of Earth, Atmospheric and Planetary Sciences, Massachusetts Institute of Technology, Cambridge,
18 MA 02139, USA

19 ⁸ Department of Chemical Engineering, Massachusetts Institute of Technology, Cambridge, MA 02139, USA

20 ^a now at: University of Chicago Laboratory Schools, Chicago, IL, USA

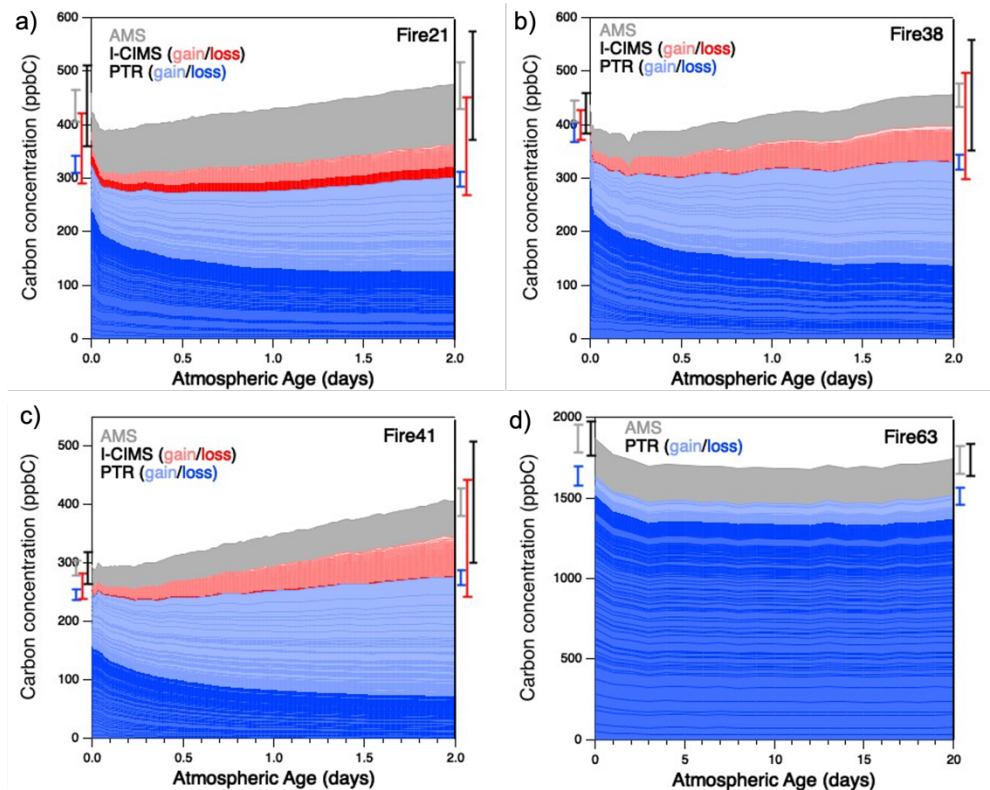
21 ^b now at: South Coast Air Quality Management District, Diamond Bar, CA 91765, USA

22 ^c now at: Tofwerk A.G., Boulder, CO, USA

23 ^d now at: Institute for Environmental and Climate Research, Jinan University, Guangzhou 511443, China

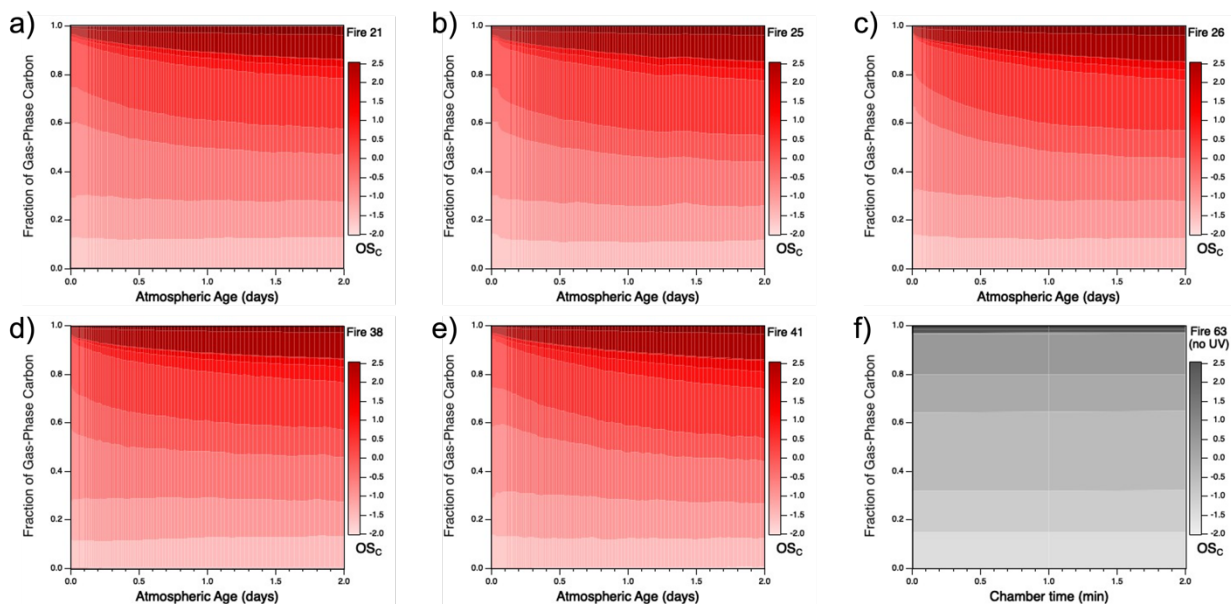
24 ^e now at: Bruker Scientific, Inc., Billerica, MA, USA
25

26 *Correspondence to:* Kevin Nihill (kevin.j.nihill@gmail.com), Jesse Kroll (jhkroll@mit.edu)

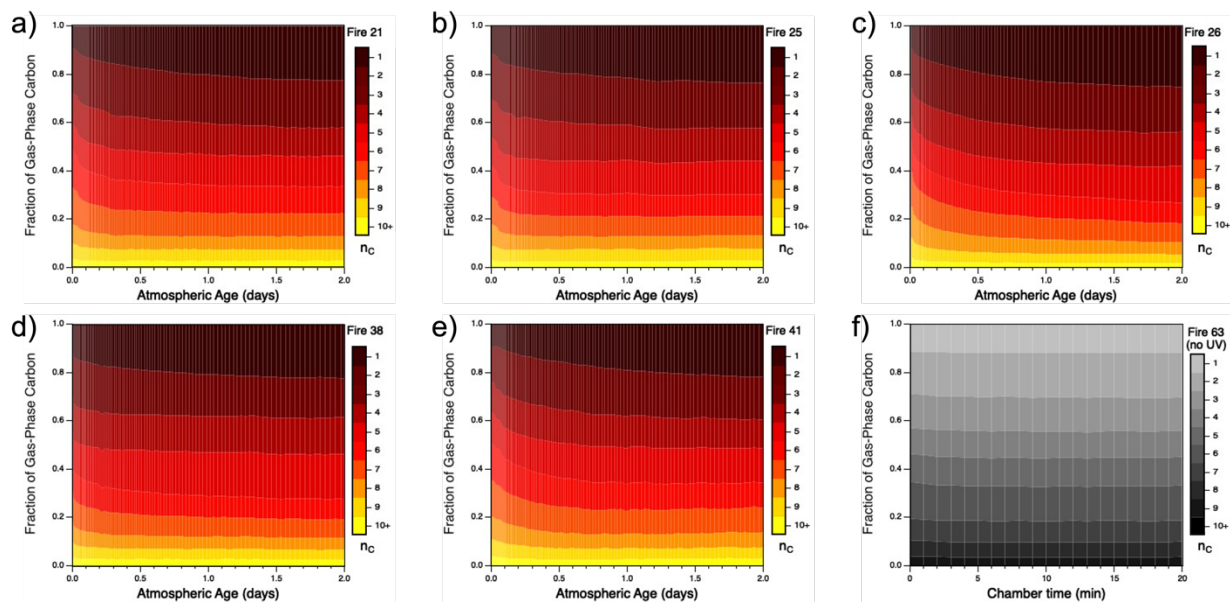


27
 28
 29
 30
 31
 32
 33
 34
 35
 36
 37

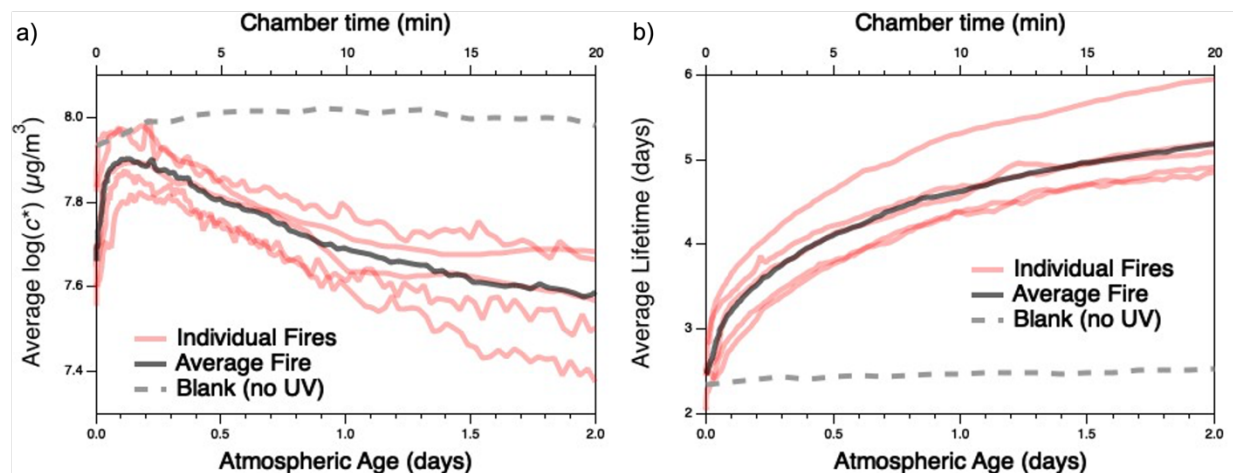
Figure S1. Measured carbon in the oxidation of emissions from (a) Fire 21 / Lodgepole Pine, litter, (b) Fire 38 / Ponderosa Pine, litter, (c) Fire 41 / Lodgepole Pine, litter, and (d) Fire 63 / blank – no UV – for Lodgepole Pine, litter. Measurements are separated into individual bands according to the instrument by which they were detected. Gas-phase measurements are separated further: blue traces represent species measured by the PTR that are primarily consumed (dark) or formed (light), ranked in order of largest decay (bottom) to largest increase (top); red traces follow the same convention, but for the I-CIMS. Fire 63 does not include I-CIMS data. The gray trace represents SOA measurements made by the AMS. The uncertainty (1σ , representing calibration uncertainties only) for each instrument is shown to the left and right of the plot, corresponding to uncertainty before and after atmospheric aging, with total uncertainty (black error bar) calculated by adding together individual uncertainties in quadrature.



38
 39 **Figure S2.** Time-evolving distribution of average carbon oxidation state (\overline{OS}_C) for gas-phase BB emissions from each
 40 of the different fuels as a function of atmospheric age (or chamber time for the blank): (a) Fire 21 / Lodgepole Pine,
 41 litter, (b) Fire 25 / Engelmann Spruce, canopy, (c) Fire 26 / Engelmann Spruce, duff, (d) Fire 38 / Ponderosa Pine,
 42 litter, (e) Fire 41 / Lodgepole Pine, litter, and (f) Fire 63 / blank – no UV – for Lodgepole Pine, litter.. Gas-phase data
 43 represented includes both PTR-MS and I-CIMS measurements, except for Fire 63, for which I-CIMS data is
 44 unavailable.
 45



46
 47 **Figure S3.** Time-evolving distribution of average carbon number (n_C) for gas-phase BB emissions from each of the
 48 different fuels as a function of atmospheric age (or chamber time for the blank): (a) Fire 21 / Lodgepole Pine, litter,
 49 (b) Fire 25 / Engelmann Spruce, canopy, (c) Fire 26 / Engelmann Spruce, duff, (d) Fire 38 / Ponderosa Pine, litter, (e)
 50 Fire 41 / Lodgepole Pine, litter, and (f) Fire 63 / blank – no UV – for Lodgepole Pine, litter. Gas-phase data represented
 51 includes both PTR-MS and I-CIMS measurements, except for Fire 63, for which I-CIMS data is unavailable.
 52



54

55

56

57

58

59

60

61

62

63

64

65

66

67

68

69

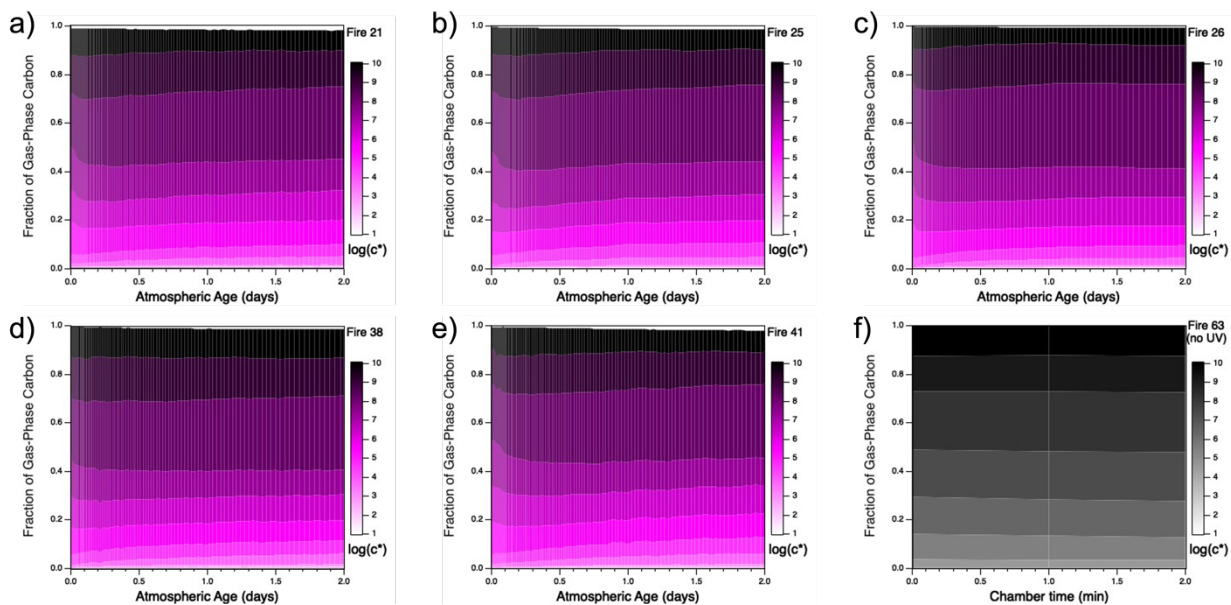
70

71

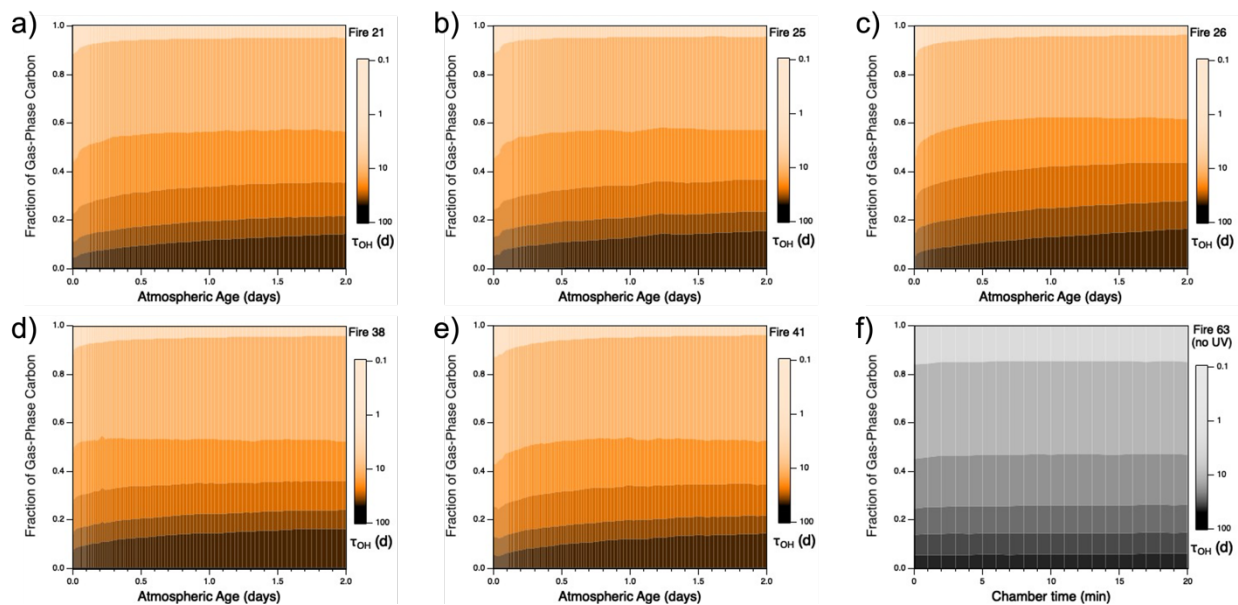
72

Figure S4. Evolution of (a) mean log of volatility (\bar{c}^*) and (b) mean oxidative lifetime ($\overline{\tau_{OH}}$) for the measured gas-phase species, as a function of atmospheric aging (or chamber time for the blank experiment). Red lines represent individual fires; gray dashed lines represent the blank run, for which only PTR data is used; black line denotes the average of all burns studied, as described in the text. Traces for individual fires are derived from the evolution of each fire's gas-phase distribution, as shown in Figs. S5-6. Values of \bar{c}^* and $\overline{\tau_{OH}}$ for unidentified species are assigned using structure-activity relationships.(Daumit et al., 2013; Donahue et al., 2013) Due to our inability to determine the functionality of N atoms in unidentified species, N is not considered in the equation for \bar{c}^* .

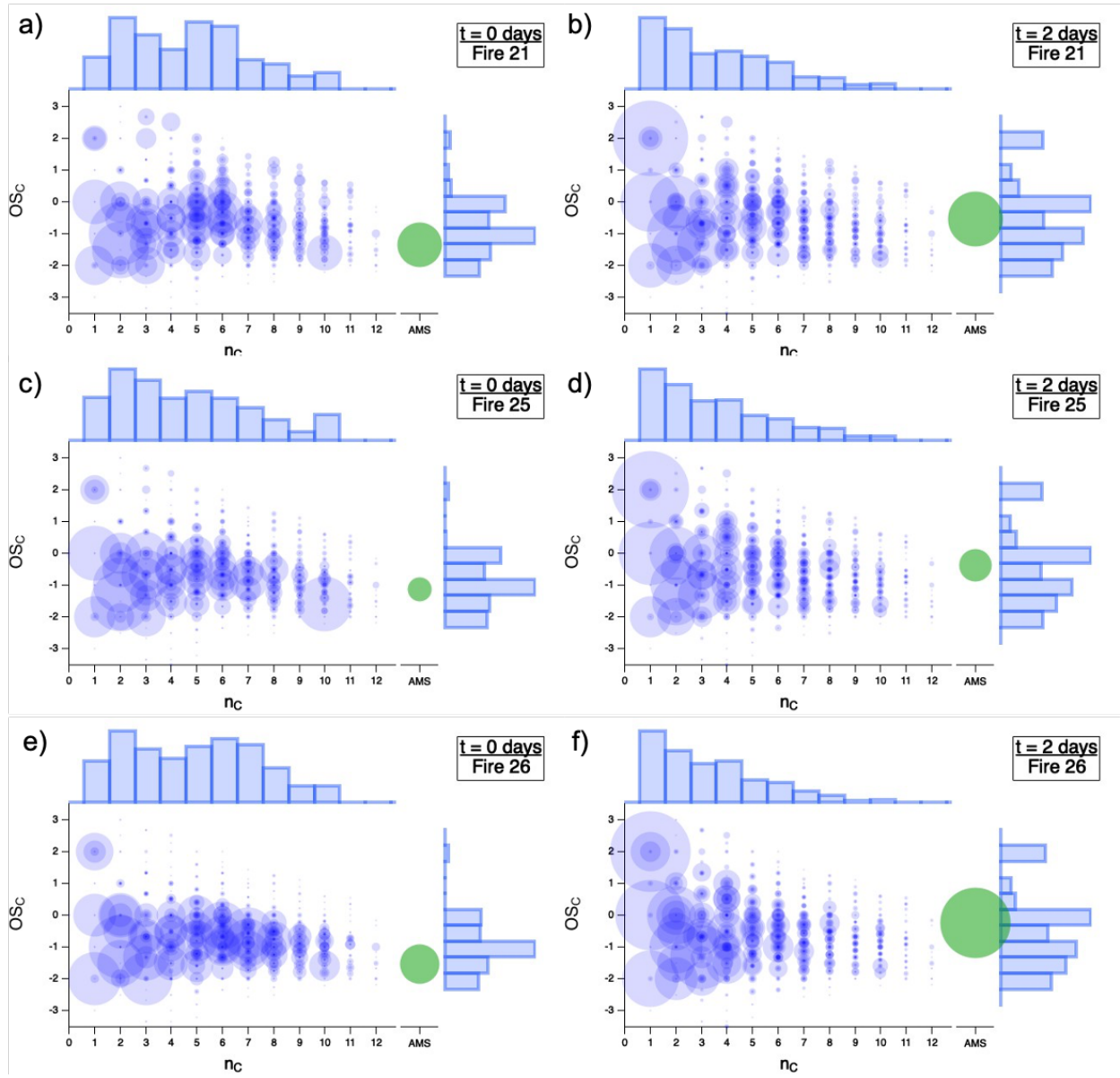
Oxidative lifetime increases with oxidation, largely due to the formation of a few long-lived species (e.g., formic acid, formaldehyde, and acetaldehyde). Volatility first spikes somewhat and then slowly decreases over the course of the experiment. These trends are somewhat different from those observed for α -pinene.(Isaacman-VanWertz et al., 2018) This difference is likely attributable to several factors. First, our study does not account for some notable classes of compounds such as CO and organic aerosol (OA), which can affect both of these metrics. Additionally, the starting materials in these two studies are rather different – our work begins with a complex mixture of reactive organic compounds with varying levels of oxidation, whereas the study of α -pinene begins with one precursor whose product distribution becomes more complex over time.

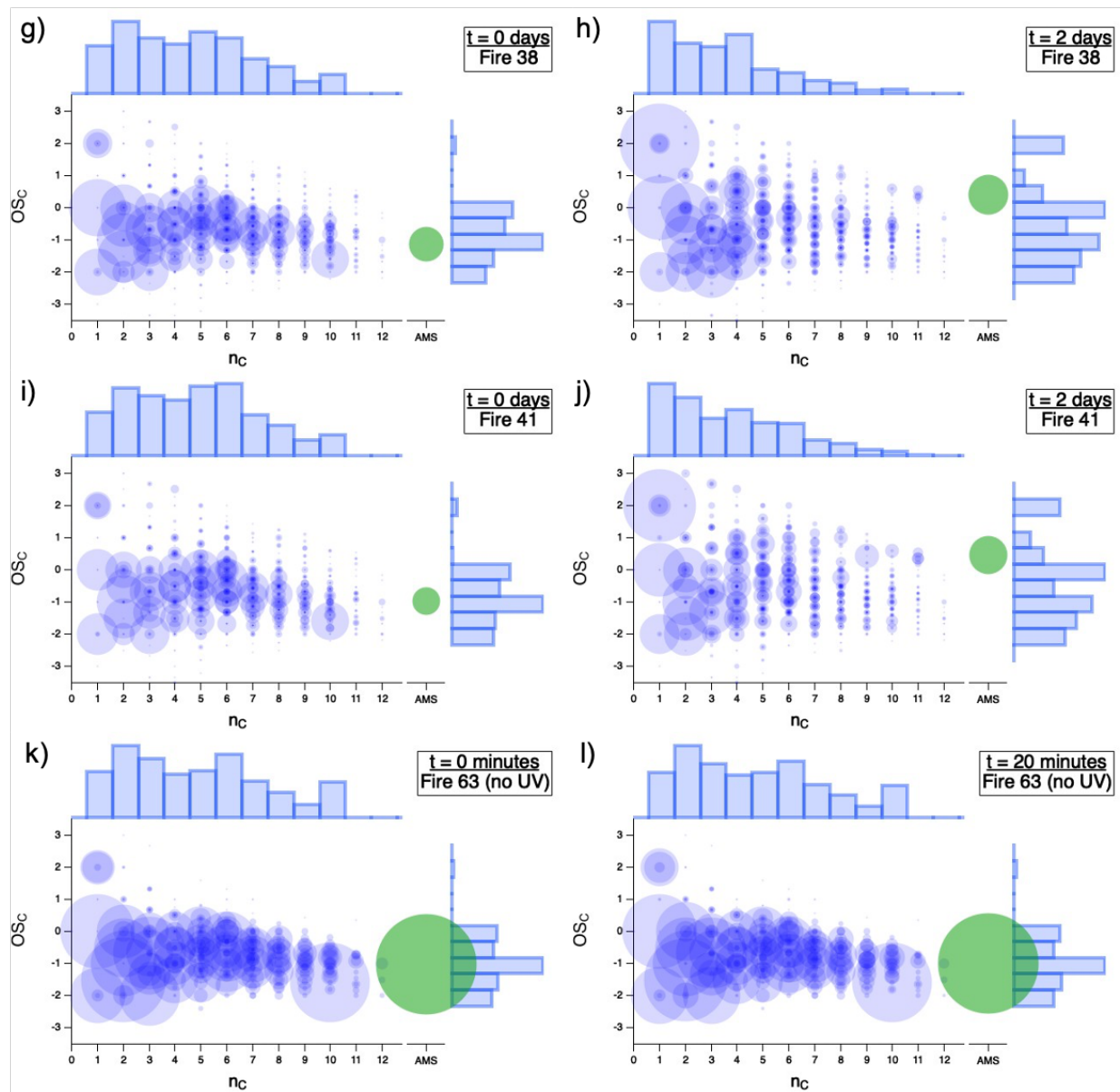


73
 74 **Figure S5.** Time-evolving distribution of average vapor pressure ($\log c^*$) for gas-phase BB emissions from each of
 75 the different fuels as a function of atmospheric age (or chamber time for the blank): (a) Fire 21 / Lodgepole Pine, litter,
 76 (b) Fire 25 / Engelmann Spruce, canopy, (c) Fire 26 / Engelmann Spruce, duff, (d) Fire 38 / Ponderosa Pine, litter, (e)
 77 Fire 41 / Lodgepole Pine, litter, and (f) Fire 63 / blank – no UV – for Lodgepole Pine, litter.. Gas-phase data
 78 represented includes both PTR-MS and I-CIMS measurements, except for Fire 63, for which I-CIMS data is
 79 unavailable.



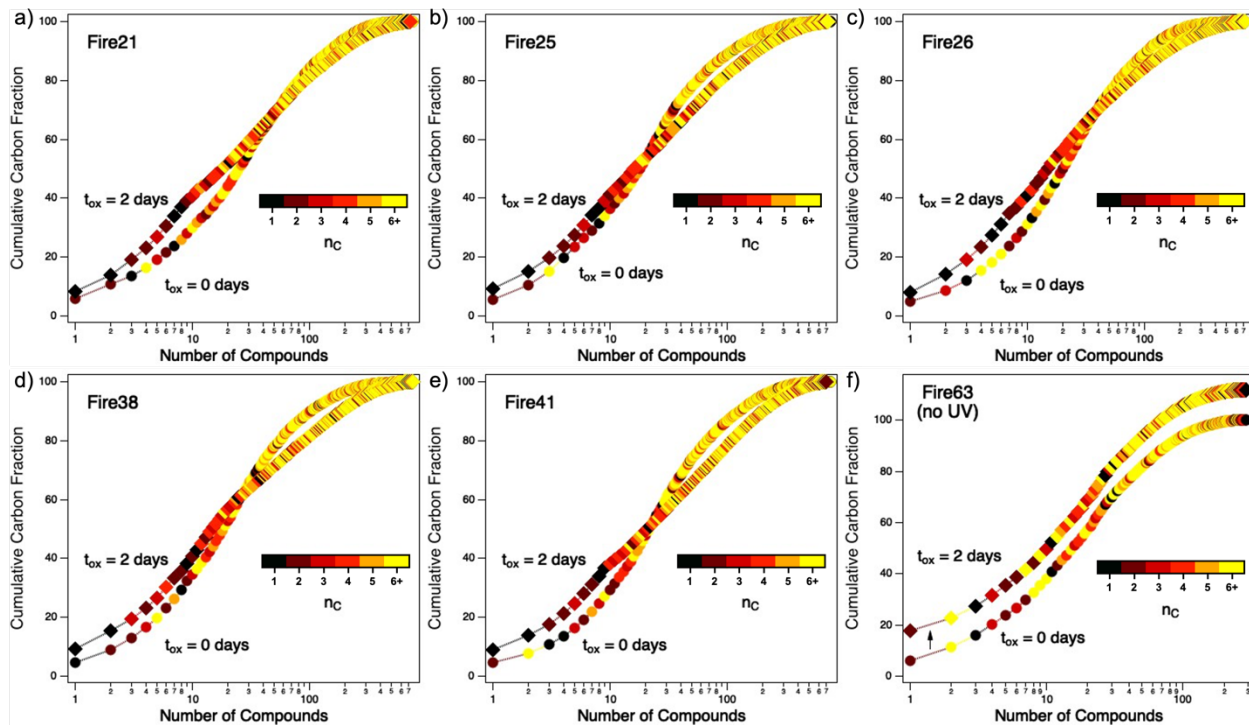
80
 81 **Figure S6.** Time-evolving distribution of average oxidative lifetime ($\overline{\tau_{OH}}$) for gas-phase BB emissions from each of
 82 the different fuels as a function of atmospheric age (or chamber time for the blank): (a) Fire 21 / Lodgepole Pine, litter,
 83 (b) Fire 25 / Engelmann Spruce, canopy, (c) Fire 26 / Engelmann Spruce, duff, (d) Fire 38 / Ponderosa Pine, litter, (e)
 84 Fire 41 / Lodgepole Pine, litter, and (f) Fire 63 / blank – no UV – for Lodgepole Pine, litter. Gas-phase data represented
 85 includes both PTR-MS and I-CIMS measurements, except for Fire 63, for which I-CIMS data is unavailable.
 86





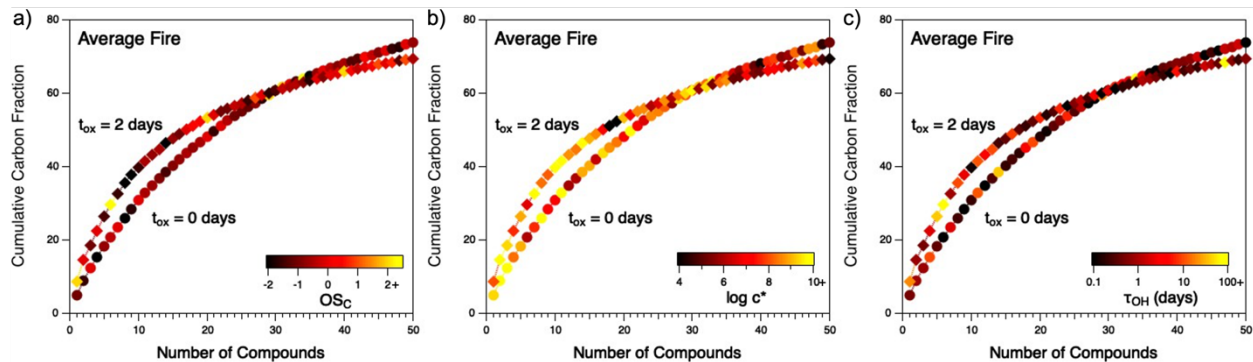
88
89
90
91
92
93
94
95
96
97
98

Figure S7. Carbon oxidation state (\overline{OS}_C) vs. carbon number (n_C) for gas-phase emissions across all fuels studied in this work: (a)-(b) Fire 21 / Lodgepole Pine, litter, (c)-(d) Fire 25 / Engelmann Spruce, canopy, (e)-(f) Fire 26 / Engelmann Spruce, duff, (g)-(h) Fire 38 / Ponderosa Pine, litter, (i)-(j) Fire 41 / Lodgepole Pine, litter, (k)-(l) Fire 63 / blank – no UV – for Lodgepole Pine, litter. Panels on the left represent freshly sampled emissions, and panels on the right show the product distribution after two days of atmosphere-equivalent oxidation (or 20 minutes of chamber time for Fire 63, the blank run). Marker area represents carbon-weighted concentration (ppbC), normalized to total carbon concentration for comparison between fuels. The separate green marker shows \overline{OS}_C and relative concentration for particle-phase measurements; the area scaling is unique from the scaling of the gas-phase data. Histograms along the top and right axes show \overline{OS}_C and n_C distributions of the gas-phase products. Gas-phase data represented includes both PTR-MS and I-CIMS measurements, except for Fire 63, for which I-CIMS data is unavailable.



99
 100
 101
 102
 103
 104
 105
 106

Figure S8. Cumulative distribution functions (CDF) showing the number of gas-phase compounds that constitute the fraction of total carbon for each individual fire for “fresh” emissions (circles) and after two days of atmosphere-equivalent aging (diamonds). Points within individual CDFs are colored by carbon number. (a) Fire 21 / Lodgepole Pine, litter, (b) Fire 25 / Engelmann Spruce, canopy, (c) Fire 26 / Engelmann Spruce, duff, (d) Fire 38 / Ponderosa Pine, litter, (e) Fire 41 / Lodgepole Pine, litter, and (f) Fire 63 / blank – no UV – for Lodgepole Pine, litter (note the vertical offset of the $t_{\text{ox}} = 2$ days trace to separate it from the otherwise overlapping “fresh” emissions trace).



107
 108 **Figure S9.** Cumulative distribution functions (CDFs) showing the percentage of gas-phase carbon for all measured
 109 compounds in the “average fire” for “fresh” emissions (circles) and after two days of atmosphere-equivalent aging
 110 (squares). Points within individual CDFs represent individual gas-phase compounds and are colored by (a) carbon
 111 oxidation state (\overline{OS}_C), (b) average vapor pressure ($\log c^*$), and (c) average oxidative lifetime ($\overline{\tau_{OH}}$).

(a)	21	25	26	38	41	63	Avg.
21	0	0.91	0.88	0.93	0.95	0.90	0.97
25		0	0.84	0.92	0.91	0.96	0.95
26			0	0.89	0.94	0.85	0.94
38				0	0.97	0.93	0.98
41					0	0.92	0.99
63						0	0.95
Avg.							0

112

(b)	21	25	26	38	41	63	Avg.
21	0	0.98	0.96	0.92	0.98	0.64	0.99
25		0	0.96	0.94	0.97	0.63	0.99
26			0	0.94	0.95	0.62	0.98
38				0	0.94	0.56	0.97
41					0	0.60	0.99
63						0	0.64
Avg.							0

113

(c)	21	25	26	38	41	63	Avg.
21	0	+0.07	+0.08	-0.01	+0.03	-0.26	+0.02
25		0	+0.12	+0.02	+0.03	-0.33	+0.04
26			0	+0.05	+0.01	-0.23	+0.04
38				0	-0.03	-0.37	-0.01
41					0	-0.32	0
63						0	-0.31
Avg.							0

114

115 **Table S1.** Absolute values of cosine similarities between gas-phase mass spectra of pairs of fires, including the
 116 “average” fire, for (a) fresh emissions and (b) after 2 days oxidative aging (or 0 to 20 minutes of chamber time for
 117 Fire 63). The difference between these two tables is represented in panel (c).
 118

Atmospheric Age = 0 Days				Atmospheric Age = 2 Days			
Compound	Frac.	nC	OsC	Compound	Frac.	nC	OsC
Acetaldehyde	4.9%	2	-1	Formic Acid	8.6%	1	2
Ethene	4.7%	2	-1.5	Formaldehyde	5.9%	1	0
Formaldehyde	3.9%	1	0	Acetaldehyde	4.0%	2	-1
Acrolein	3.3%	3	-0.67	Acetic Acid	4.0%	2	0
Methanol	3.0%	1	-2	Acetone	3.8%	3	-1.33
Acetic Acid	2.8%	2	0	Isocyanic Acid	3.1%	1	4
Propene	2.6%	3	-2	Ethene	3.1%	2	-1.5
MethylFurfural/Benzenediol	2.2%	6	-0.33	Methanol	2.9%	1	-2
Monoterpenes	2.2%	10	-1.6	Ethanol	2.4%	2	-2
Acetylene	2.1%	2	-0.5	1,3-Butadiene	2.0%	4	-1.5
Acetone	2.0%	3	-1.33	Acetylene	1.7%	2	-0.5
Guaiacol	1.8%	7	-0.57	Hydroxyacetone/Methylacetate	1.6%	3	-0.67
Furan	1.8%	4	-0.5	2,3-Butanedione	1.6%	4	-0.5
Cresol	1.8%	7	-0.86	Propene	1.6%	3	-2
Methylfuran	1.8%	5	-0.8	Acrolein	1.3%	3	-0.67
Furfural	1.7%	5	0	Methylpropanoate	1.3%	4	-1
Hydroxyacetone/Methylacetate	1.6%	3	-0.67	Methylglyoxal/Acrylic Acid	1.2%	3	0
Phenol	1.6%	6	-0.67	C4H6O4	1.0%	4	0.5
1,3-Butadiene	1.6%	4	-1.5	Dihydrofuran-dione/Succinic Anhydride	1.0%	4	0.5
2,3-Butanedione	1.6%	4	-0.5	Hydrogen Cyanide	1.0%	1	2
Furanone/Unsaturated Carbonyls	1.5%	4	0				
Methylglyoxal/Acrylic Acid	1.4%	3	0				
Benzene	1.4%	6	-1				
2-Methanolfuran	1.4%	5	-0.4				
Formic Acid	1.3%	1	2				
MVK/MACR	1.3%	4	-1				
Toluene	1.2%	7	-1.14				
Isoprene	1.1%	5	-1.6				
Methylguaiacol	1.1%	8	-0.75				
Hydrogen Cyanide	1.0%	1	2				
Dimethylfuran	1.0%	6	-1				

119
120
121
122
123
124
125

Table S2. List of gas-phase compounds that constitute $\geq 1.0\%$ of carbon concentration in the reaction mixture for the “average fire” before (left) and after (right) two days of atmosphere-equivalent oxidation. Compound name, fraction of total gas-phase concentration, carbon number, and average carbon oxidation state are listed for each compound. Arrows indicate change in concentration after aging, with red arrows representing a decrease, blue arrows representing an increase, and black arrows representing no change.

126 **References**

127

128 Daumit, K. E., Kessler, S. H., and Kroll, J. H.: Average chemical properties and potential formation pathways of
129 highly oxidized organic aerosol, *Faraday Discuss.*, 165, 181, <https://doi.org/10.1039/c3fd00045a>, 2013.

130

131 Donahue, N. M., Chuang, W., Epstein, S. A., Kroll, J. H., Worsnop, D. R., Robinson, A. L., Adams, P. J., and
132 Pandis, S. N.: Why do organic aerosols exist? Understanding aerosol lifetimes using the two-dimensional volatility
133 basis set, *Environ. Chem.*, 10, 151–157, <https://doi.org/10.1071/EN13022>, 2013.

134

135 Isaacman-VanWertz, G., Massoli, P., O'Brien, R., Lim, C. Y., Franklin, J. P., Moss, J. A., Hunter, J. F., Nowak, J.
136 B., Canagaratna, M. R., Misztal, P. K., Arata, C., Roscioli, J. R., Herndon, S. T., Onasch, T. B., Lambe, A. T.,
137 Jayne, J. T., Su, L., Knopf, D. A., Goldstein, A. H., Worsnop, D. R., and Kroll, J. H.: Chemical evolution of
138 atmospheric organic carbon over multiple generations of oxidation, *Nat. Chem.*, 10, 1–7,
139 <https://doi.org/10.1038/s41557-018-0002-2>, 2018.

140